Check for updates

International Journal of Mechanical System Dynamics

WILEY

IJMSD International Journal of Mechanical System Dynamics Open Access

RESEARCH ARTICLE OPEN ACCESS

Dynamic Characteristics of Vibrating Flip-Flow Screens Considering Material Impact Force

Boyu Wu[1,2,3] | Shuqian Cao[1,2,3] | Qingquan Luo[1,2,3]

[1]School of Mechanical Engineering, Tianjin University, Tianjin, China | [2]Tianjin Key Laboratory of Nonlinear Dynamics and Control, Tianjin, China | [3]National Key Laboratory of Vehicle Power System, Tianjin, China

Correspondence: Shuqian Cao (sqcao@tju.edu.cn)

Received: 27 December 2024 | **Revised:** 17 February 2025 | **Accepted:** 1 March 2025

Funding: This study was supported by the National Natural Science Foundation of China (Grant No. 12272259).

Keywords: dynamic characteristics | impact force | material motion | vibrating flip-flow screen

ABSTRACT

Vibrating flip-flow screens are widely used in the field of screening; its actual operation is affected by the impact force of materials, but existing research usually ignores this effect. Based on this background, considering the influence of material impact force and moment on vibrating flip-flow screens, this paper develops a dynamic model and a vibration differential equation of a vibrating flip-flow screen, performs the analysis of material movement and calculation of the material impact force, and includes the material impact force in the dynamic characteristic analysis of a vibrating flip-flow screen. The results indicate the following: (1) The impact forces F_x and F_y account for 29% and 57.58% of the excitation force amplitude, respectively, indicating that they are of the same magnitude as the excitation force. Material impact increases the vibration amplitudes of the main and floating frames, and therefore, cannot be ignored in vibrating flip-flow screen design. (2) By comparing the vibrating flip-flow screen's responses with and without the impact, it is found that impact force significantly influences the system response, causing the displacement curve to shift and the amplitude–frequency curve to have periodic fluctuations and peak values. (3) The effects of impact parameters on the dynamic characteristics of a vibrating flip-flow screen are studied. The results show that increases in material mass and material binding coefficient lead to a decrease in the system natural frequencies. Due to the impact force, the amplitude–frequency curve of the main frame peaks at a frequency lower than the first order of the natural frequency, and the amplitude–frequency curve of the floating frame peaks in the intervals of 5–10 Hz and 20–25 Hz. The results provide a theoretical reference for the design of vibrating flip-flow screens. The operating frequency of vibrating flip-flow screens should be selected to avoid the peak value due to the impact force, which helps extend the working life.

1 | Introduction

In screening operations, the wet fine-grained material sticks easily and difficult to screen because of its high water content and small particle size. Due to the periodic motion of the elastic screen, the acceleration of a vibrating flip-flow screen is much higher than that of an ordinary vibrating screen, and the projectile acceleration of the screen can reach 30–50 times the gravitational acceleration. The material bounces on the screen after making contact with the screen, which can effectively prevent the retention and adhesion of the material onto the screen or material blocking the screen mesh. Therefore, the screening problem of wet fine-grained materials can be better solved with the use of a flip-flow screen [1, 2].

Material is an important factor that cannot be ignored when studying the dynamic characteristics of a vibrating flip-flow screen. Due to the complexity of the movement of the material

This is an open access article under the terms of the Creative Commons Attribution License, which permits use, distribution and reproduction in any medium, provided the original work is properly cited.

© 2025 The Author(s). *International Journal of Mechanical System Dynamics* published by John Wiley & Sons Australia, Ltd on behalf of Nanjing University of Science and Technology.

on the screen, the material is often ignored in many studies or is considered as the equivalent mass for system dynamics analysis [3–6]. However, in the work of a vibrating flip-flow screen, the material has an impact on the screen surface due to the throwing motion of the vibrating flip-flow screen and has obvious nonlinear characteristics, so it has an important influence on the dynamic characteristics of the vibrating flip-flow screen.

Some scholars have conducted relevant research on the impact force produced by materials. He et al. [7] developed a coupling analysis model of vibration system dynamics and particle dynamics, taking into account the throwing effect of the screen body on the material, and studied the change law of the material impact force with the main parameters of the vibrating screen. The relationships between the screen surface area, the screen length, the screen surface inclination angle, and the vibration direction angle and material impact force are determined. Wang et al. [8] designed the orthogonal test, used range and variance analysis to determine the impact of vibration parameters on the impact force, and used the discrete finite element method to study the structural response of the screen under the impact of materials. Zhou et al. [9] analyzed the nonlinear force acting on the screen surface when the material is thrown on the large linear screen, and on this basis, determined the formula for calculating the equivalent mass and equivalent damping of the material. Manuel Moncada et al. [10] developed a 3DOF model of a vibrating screen and found that the amplitude calculated without considering the impact force of the material was inaccurate.

Many scholars have conducted relevant studies on the effect of material impact force on various aspects of vibrating screens [11, 12]. Hou et al. [13] proposed a simplified mechanical model considering material impact for a self-synchronous vibration system driven by two eccentric rotors and obtained the change law of phase difference affected by material impact. Jiao et al. [14] studied the influence of material impact force on a double-mass vibrating screen and analyzed the amplitude–frequency response of the upper and lower bodies. Ma [15] considered the influence of friction force and impact force of materials on a double-mass linear vibrating screen and found that the amplitude of the upper body decreases while that of the lower body increases when the impact force of materials is considered. Xia et al. [16] studied the dynamic response of linear screens under material impact by developing a discrete element method-multi body kinematics coupling model. Li et al. [17] developed a time-varying piece-based nonlinear dynamic model of an elliptical vibrating screen based on the force analysis of the material under sliding and throwing motion and obtained an approximate steady-state analytical solution of the system using the incremental harmonic balance method. Lin et al. [18] studied the influence of materials on the equivalent stiffness and equivalent damping of screens by dynamic tests. Peng et al. [19] tested and analyzed the vibration and strain signals of the screen, studied the dynamic influence of coal on a vibrating screen, analyzed the mechanical characteristics of the load-bearing beam, and found that the structural strain increased by 14.79% after considering the influence of materials. It has been observed that the material in practical engineering has a significant effect on the vibrating screen, and if such an effect is not considered, the numerical and experimental results deviate significantly.

Based on this background, the effect of the impact force generated by the material on a vibrating screen is clear. At present, more attention is paid to the effect of the material impact force on the linear screen, while there is a lack of relevant research on vibrating flip-flow screens due to the complexity of their material movement. Moreover, most of the previous studies focus on the effect of vibration parameters on the impact force and the structural response of the impact force on the screen, and there is a lack of research on the dynamic characteristics of vibrating flip-flow screens. In this paper, a dynamic model of a vibrating flip-flow screen considering the impact force of the material is developed, the impact force and impact moment generated by the material on the vibrating flip-flow screen are determined, and the effects of the impact parameters on the dynamic characteristics of the vibrating flip-flow screen are analyzed, which can make the dynamic model closer to the actual system and help to guide the design and improvement of vibrating flip-flow screens.

2 | Model of a Vibrating Flip-Flow Screen

In the dynamic analysis modeling of a vibrating flip-flow screen, the displacement in the compression direction of the shear spring between the floating frame and the main frame is usually ignored, and only its displacement along the moving direction of the floating frame is studied. However, the compression direction of the shear spring should not be ignored in the actual analysis. Therefore, taking shear rubber springs with Shore hardness of 50HS as an example, the analysis is as follows:

The relationship between the tensile modulus E and the shear modulus G of the rubber spring and Shore hardness HS are expressed, respectively, [20] as follows:

$$E = 3.57e^{0.033HS}, \tag{1}$$

$$G = 1.19e^{0.033HS}. \tag{2}$$

The three-dimensional model and dimensions of the shear spring are shown in Figure 1.

For a rectangular section, when the shear deformation direction is parallel to the longitudinal side, the shear shape coefficient is given by

$$q = \frac{1}{1 + \frac{G}{E}\left(\frac{h}{a}\right)^2}, \tag{3}$$

where a denotes the length of the rubber spring and h is the height of the rubber spring.

Without considering the effects of cross-sectional area variations and bending deformation, the stiffness k_x in the shear

27671402, 2025, 3, Downloaded from https://onlinelibrary.wiley.com/doi/10.1002/msd2.70010 by CochraneChina, Wiley Online Library on [11/12/2025]. See the Terms and Conditions (https://onlinelibrary.wiley.com/terms-and-conditions) on Wiley Online Library for rules of use; OA articles are governed by the applicable Creative Commons License

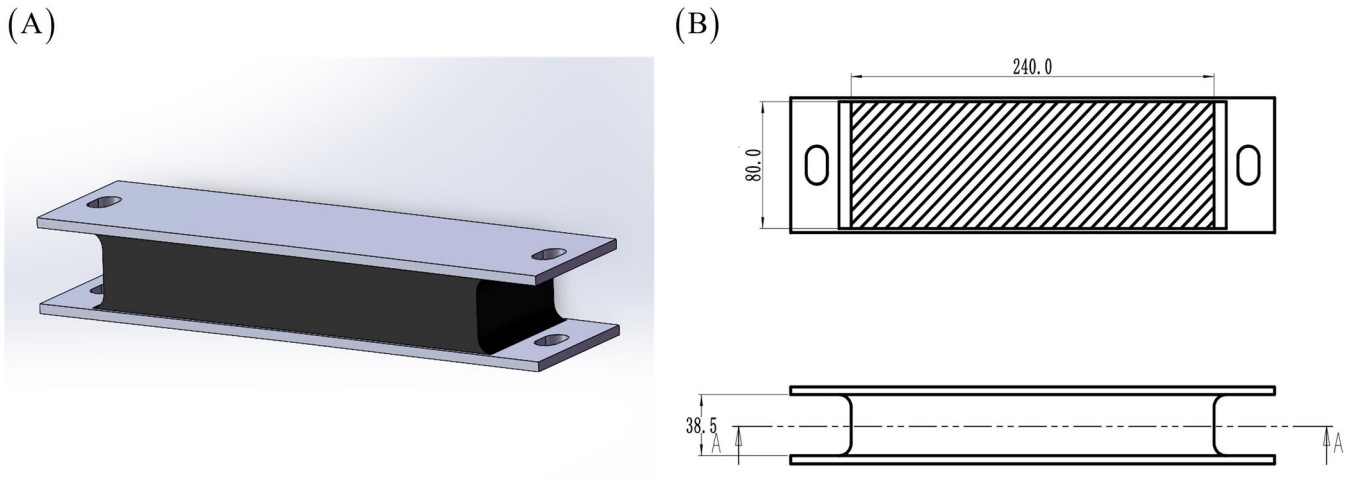

FIGURE 1 | Three-dimensional model and dimensions of shear spring: (A) Three-dimensional model of the shear spring. (B) Dimensions of the shear spring.

direction of the shear rubber spring is determined using the following approximate formula:

$$k_x = \frac{F_x}{x} = \frac{A_F G q'}{h}, \tag{4}$$

where F_x is the shear force, A_F is the cross-sectional area, x is the deformation of the rubber spring in the direction of the shear force, and q' is the shear shape coefficient.

The stiffness k_y in the compression direction of the shear rubber spring is determined as follows: Under compression conditions, the elastic modulus of the rubber spring is influenced by its shape, size, and the combination state of the supporting surface of the attachment. Consequently, the elastic modulus of the rubber spring differs from that of the rubber material itself. Direct use of the elastic modulus of the rubber material would result in significant errors. The elastic modulus E' of the rubber spring is related to the elastic modulus E of the rubber material as follows [21]:

$$E' = KE, \tag{5}$$

where K is the compression shape factor of the spring.

For a rectangular rubber spring, the compression shape coefficient K is defined as

$$K = 1.2(1 + 2.22\varphi^2), \tag{6}$$

where φ is the area ratio

$$\varphi = \frac{A_F}{A_Z} = \frac{ab}{2(a+b)h}, \tag{7}$$

where b represents the width of the rubber spring, h is the height of the rubber spring, and A_Z is the free area of the side surface of the rubber spring. Therefore, the compression stiffness K_y of the shear rubber spring can be determined from

$$k_y = \frac{F_y}{y} = KEA_F \frac{1}{h}\left(1 + \frac{y}{h}\right). \tag{8}$$

In the case of small deformation, the elastic force is approximately linear, and an approximate spring stiffness formula can be written as

$$k_y = KEA_F \frac{1}{h}. \tag{9}$$

In this paper, the shear spring parameters are as follows: $a = 240$ mm, $b = 80$ mm, $h = 40$ mm, $E = 1.8$ MPa, and $G = 0.6$ MPa. According to Equations (4), (6), (7), and (9), shear stiffness of the shear spring $K_x = 296.68$ kN/m and compression stiffness $K_y = 2529.2$ kN/m can be obtained.

By comparing the shear stiffness K_x and the compression stiffness K_y of the shear spring, it can be seen that the compression stiffness of the shear spring is only 8.525 times that of the shear stiffness, which means that they are of the same order. Therefore, the vertical and parallel motion of the floating frame relative to the main frame should be considered in the dynamic modeling analysis of the vibrating flip-flow screen.

The dynamic model of the vibrating flip-flow screen used in this study is shown in Figure 2. The vibrating flip-flow screen is composed of the main frame m_1, the floating frame m_2, and two eccentric rotors with mass m_0. The main frame m_1 is connected to the frame mounted on the ground by vibration isolation springs and the floating frame m_2 is connected to the main frame m_1 by rubber shear spring and flip-flow screen panels. A pair of eccentric rotors m_0 driven by the motor is symmetrically mounted on the main frame; l_1 is the distance of the line of action of the excitation force generated by the rotors from the centroid of the main frame and l_2 represents the horizontal distance from the center of the main frame to the isolation spring at one end. The dispersed impact force of the material is considered as the concentrated force F_1 acting on the center of mass of the floating frame and the moment M_1 acting on the center of mass of the main frame.

27671402, 2025, 3, Downloaded from https://onlinelibrary.wiley.com/doi/10.1002/msd2.70010 by CochraneChina, Wiley Online Library on [11/12/2025]. See the Terms and Conditions (https://onlinelibrary.wiley.com/terms-and-conditions) on Wiley Online Library for rules of use; OA articles are governed by the applicable Creative Commons License

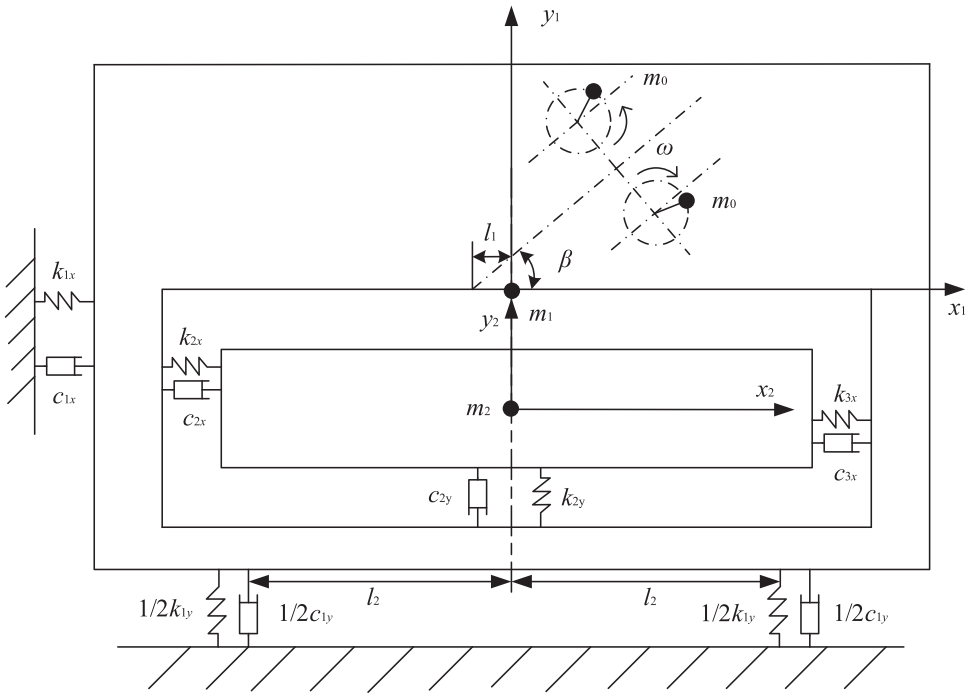

FIGURE 2 | 5 DOF Dynamics model of a vibrating flip-flow screen.

The displacement of the main frame along the horizontal direction is x_1, the displacement of the main frame perpendicular to the flip-flow screen panel upward is y_1, the angle of rotation about the axis through the center of mass perpendicular to the side plate is φ, and the displacement of the floating frame relative to the main frame along the horizontal direction is x_2. The displacement of the floating frame relative to the main frame perpendicular to the horizontal direction is y_2. That is, $\boldsymbol{q} = [x_1, y_1, x_2, y_2, \varphi]^{\mathrm{T}}$ is the vector of generalized coordinates of the system.

The total kinetic energy of the vibrating flip-flow screen system can be expressed as

$$T = \frac{1}{2}m_1(\dot{x}_1^2 + \dot{y}_1^2) + \frac{1}{2}J_1\dot{\varphi}^2 + \frac{1}{2}m_2(\dot{x}_1 + \dot{x}_2)^2 + \frac{1}{2}m_2(\dot{y}_1 + \dot{y}_2)^2, \tag{10}$$

where m_1 represents the mass of the main frame, m_2 is the mass of the floating frame, and J_1 denotes the moment of inertia of the screen body around the axis perpendicular to $x_1 o_1 y_1$.

The total elastic potential energy of the vibration system is as follows:

$$V = \frac{1}{2}k_{1x}x_1^2 + \frac{1}{2}k_{1y}\left(y_1^2 + \varphi^2 l_2^2\right) + \frac{1}{2}k_{2x}x_2^2 + \frac{1}{2}k_{2y}y_2^2 + \frac{1}{2}k_{3x}x_2^2, \tag{11}$$

where k_{1x} is the equivalent stiffness of the isolation spring along the x_1 direction, k_{1y} is the equivalent stiffness of the isolation spring along the y_1 direction, k_{2x} represents the shear stiffness of the shear spring along the x_2 direction, k_{2y} indicates the compression stiffness of the shear spring along the y_2 direction, k_x is the horizontal stiffness of the isolation spring, and k_y denotes the vertical stiffness of the isolation spring.

The dissipated energy of the vibration system is given by

$$D = \frac{1}{2}c_{1x}\dot{x}_1^2 + \frac{1}{2}c_{1y}\left(\dot{y}_1^2 + \dot{\varphi}^2 l_2^2\right) + \frac{1}{2}(c_{2x} + c_{3x})\dot{x}_2^2 + \frac{1}{2}c_{2y}\dot{y}_2^2, \tag{12}$$

where c_{1x} and c_{1y} represent the damping coefficients of the isolation spring along the x and y directions, respectively, c_{2x} and c_{2y} are the damping coefficients of the shear spring along the x and y directions, respectively, and c_{3x} is the damping coefficient of flip-flow screen panels.

The excitation force generated by the eccentric block group driven by the motor in reverse operation is represented as

$$P = A\sin\omega t, \tag{13}$$

where A is the amplitude of the excitation force and ω is the circular frequency of the excitation force.

By substituting the kinetic energy, potential energy, and dissipative energy of the system into a Lagrange equation, the dynamic equations of the system can be written as

$$\boldsymbol{M\ddot{q}} + \boldsymbol{C\dot{q}} + \boldsymbol{Kq} = \boldsymbol{F}, \tag{14}$$

where $\boldsymbol{M}$, $\boldsymbol{K}$, $\boldsymbol{C}$, and $\boldsymbol{F}$ are the system-generalized mass matrix, the damping matrix, the stiffness matrix, and the generalized force vector, respectively, defined as follows:

27671402, 2025, 3, Downloaded from https://onlinelibrary.wiley.com/doi/10.1002/msd2.70010 by CochraneChina, Wiley Online Library on [11/12/2025]. See the Terms and Conditions (https://onlinelibrary.wiley.com/terms-and-conditions) on Wiley Online Library for rules of use; OA articles are governed by the applicable Creative Commons License

$$\boldsymbol{M}=\begin{bmatrix} m_1+m_2 & 0 & m_2 & 0 & 0 \\ 0 & m_1+m_2 & 0 & m_2 & 0 \\ m_2 & 0 & m_2 & 0 & 0 \\ 0 & m_2 & 0 & m_2 & 0 \\ 0 & 0 & 0 & 0 & J_1 \end{bmatrix}, \tag{15}$$

$$\boldsymbol{K}=\begin{bmatrix} k_{1x} & & & & \\ & k_{1y} & & & \\ & & k_{2x}+k_{3x} & & \\ & & & k_{2y} & \\ & & & & k_{1y}l_2^{\,2} \end{bmatrix}, \tag{16}$$

$$\boldsymbol{C}=\begin{bmatrix} c_{1x} & 0 & 0 & 0 & 0 \\ 0 & c_{1y} & 0 & 0 & 0 \\ 0 & 0 & c_{2x}+c_{3x} & 0 & 0 \\ 0 & 0 & 0 & c_{2y} & 0 \\ 0 & 0 & 0 & 0 & c_{1y}l_2^{\,2} \end{bmatrix}, \tag{17}$$

$$\boldsymbol{F}=\begin{bmatrix} P\cos\beta+\dfrac{F_x}{2} & P\sin\beta+\dfrac{F_y}{2} & \dfrac{F_x}{2} & \dfrac{F_y}{2} & -Pl_1+M_1 \end{bmatrix}^{\mathrm{T}}, \tag{18}$$

where k_{3x} is the total stiffness of flip-flow screen panels and F_x and F_y represent the components of the material impact force in the x_2 and y_2 directions, respectively. M_1 is the impact torque of the material on the floating frame of the vibrating flip-flow screen.

3 | Analysis of Material Motion on the Screen

The motion of the material on the screen exists in various forms, such as throwing motion, relative stationary motion, forward sliding, and reverse sliding. The main motion of the material is the throwing motion. Csizmadia et al. [22] simulated the throwing motion of the material on the screen using a single spherical material.

3.1 | Calculation of the Initial Material Speed

In the absolute coordinate system xoy, the absolute coordinate system axis x is parallel to the ground and axis y is perpendicular to the ground. By analyzing the actual motion of the vibrating flip-flow screen, it can be seen that the initial velocity of the material on the screen is divided into two parts, namely, the velocity v_2 of the floating frame and the velocity v_3 generated by the flip-flow screen panel, as shown in Figure 3.

The displacement formula of the floating frame is as follows:

$$x_{F2}=B\sin\omega t, \tag{19}$$

where B is the amplitude of the displacement curve of the floating frame and t represents the time. The velocity of the floating frame along the direction of the excitation force can be obtained from the equation

$$v_2=B\omega\cos\omega t. \tag{20}$$

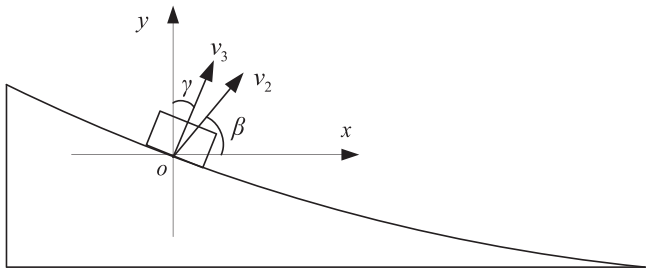

FIGURE 3 | Initial velocity composition diagram of material.

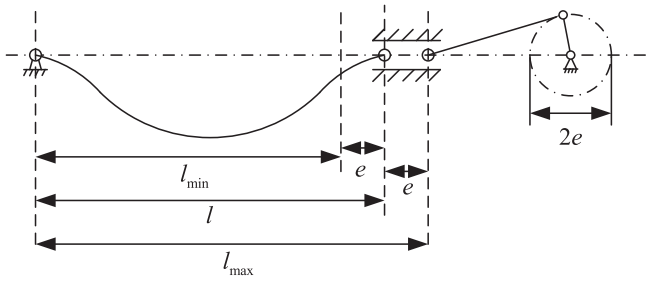

FIGURE 4 | Simplified model of screen panel motion.

The velocity of the material at the beginning of the throwing motion can be obtained from

$$\begin{cases} v_{x0}=v_2\cos\beta+v_3\sin\gamma \\ v_{y0}=v_2\sin\beta+v_3\cos\gamma \end{cases}, \tag{21}$$

$$v_0=\sqrt{v_{x0}^2+v_{y0}^2}, \tag{22}$$

where β is the angle between v_2 and the horizontal plane and γ is the angle between v_3 and the vertical plane.

The acceleration of throwing motion is caused by the flip-flow screen panel. This acceleration is driven by the periodic bending motion of the beam on the screen frame. The motion of each screen panel is similar, and, therefore, the motion of the entire screen surface can be derived by studying a single screen panel. Taking one unit of the screen surface in the screen panel, simplifying it as a movable end and a fixed end of a simply supported beam, and assuming that the length of the screen surface is independent of the bending radius and in the no-load condition, the screen surface deflection curve can be replaced by three consecutive arcs, as shown in Figure 4.

Therefore, when any screen panel is simplified into a simply supported beam, the expressions of displacement, velocity, and acceleration at the center point of the screen panel can be given by [23, 24]

$$\begin{aligned} z(x,t)&=\frac{1}{\pi}\sqrt{8el(1+\cos\omega t)}, \\ v(x,t)&=z'(x,t)=-\frac{\omega}{2\pi}\sqrt{\frac{8el}{1+\cos\omega t}}\sin\omega t, \\ a(x,t)&=z''(x,t)=-\frac{\omega^2}{2\pi}\sqrt{8el}\left[\frac{\sin^2\omega t}{2(1+\cos\omega t)^{\frac{3}{2}}}-\frac{\cos\omega t}{\sqrt{1+\cos\omega t}}\right], \end{aligned} \tag{23}$$

27671402, 2025, 3, Downloaded from https://onlinelibrary.wiley.com/doi/10.1002/msd2.70010 by CochraneChina, Wiley Online Library on [11/12/2025]. See the Terms and Conditions (https://onlinelibrary.wiley.com/terms-and-conditions) on Wiley Online Library for rules of use; OA articles are governed by the applicable Creative Commons License

where e represents eccentricity and l denotes the screen panel length.

The focus of this study is on the whole vibrating flip-flow screen, so the acceleration at the middle point of the screen panel is considered as the peak acceleration of screen panels. The acceleration at the middle point of the screen panel presents a cosine distribution with time and the screen panel force on the material is always perpendicular to the sieve plate upward. Therefore, the material acceleration is simplified as follows:

$$a(t) = \frac{T}{2}(\cos \omega t + |\cos \omega t|), \tag{24}$$

where T is the amplitude of acceleration at the middle point of the screen panel.

Thus, the velocity v_3 provided to the material by the screen panel is given by

$$v_3 = \int_t^{t+t_1} a(t)\mathrm{d}t = \int_t^{t+t_1} \frac{T}{2}(\cos \omega t + |\cos \omega t|), \tag{25}$$

where t_1 is the single working time of the flip-flow screen panel.

The angle θ between the initial velocity v_0 of the material throwing motion and the horizontal direction can be calculated using the following formula:

$$\theta = \arctan\left(\frac{v_{y0}}{v_{x0}}\right). \tag{26}$$

The velocity v_2 of the floating frame to the material on the screen changes little with time compared with the velocity v_3 of the screen surface, so only the change of angle θ caused by v_3 is considered. The angle θ between the initial velocity v_0 of the material slant motion and the horizontal direction changes with time t, as shown in Figure 5.

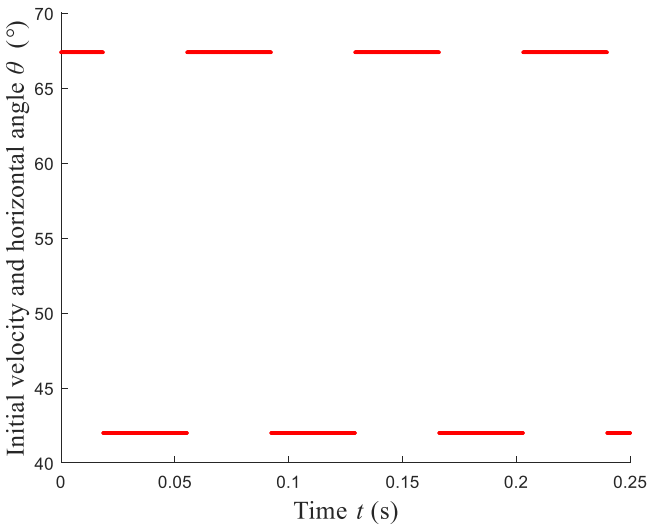

FIGURE 5 | Angle θ changes with time.

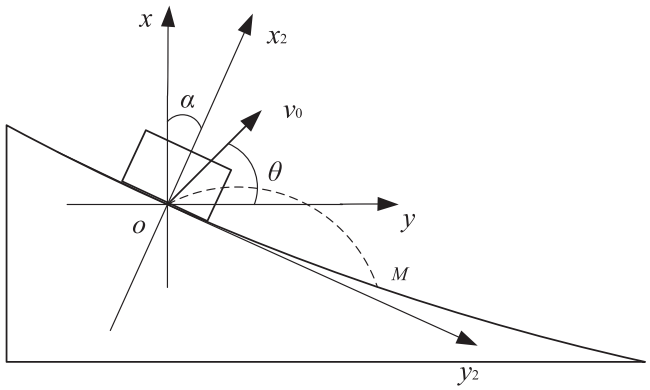

FIGURE 6 | Material throwing process.

3.2 | Analysis of the Material Throwing Process

The discharge end of the floating frame is tangential to the horizontal plane, and the angle between the material movement direction and the horizontal plane is θ. The object coordinate system is x_2oy_2 with axis x_2 tangential to the screen plane and axis y_2 perpendicular to the section plane. The angle between the absolute coordinate system and the object coordinate system is α, as shown in Figure 6.

The material begins to move at an initial velocity of v_0 relative to the ground and falls to point M. Therefore, the motion of the material can be decomposed in the absolute coordinate system and the object coordinate system, respectively, as

$$\begin{cases} v_{x1} = v_0 \cos\theta \\ v_{y1} = v_0 \sin\theta \end{cases}, \begin{cases} v_{x2} = v_0 \cos(\alpha + \theta) \\ v_{y2} = v_0 \sin(\alpha + \theta) \end{cases}. \tag{27}$$

Assuming that the throwing time of the material is t_2, the displacement of the material in the absolute coordinate system is a in the x_1 axis direction and b in the y_1 axis direction. The displacement of the material in the object coordinate system x_2 axis direction is c and the displacement in the y_2 axis direction is d. When analyzed separately in the absolute coordinate system and the object coordinate system, the following formula can be obtained:

$$\begin{cases} a = v_{x1}t_2 \\ b = -v_{y1}t_2 + \frac{1}{2}gt_2{}^2 \end{cases}, \begin{cases} c = v_{x2}t_2 + \frac{1}{2}a_3t_2^2 \\ d = -v_{y2}t_2 + \frac{1}{2}a_4t_2^2 \end{cases}, \tag{28}$$

where $a_3 = g\sin\alpha$ and $a_4 = g\cos\alpha$. The simultaneous solution yields the material throwing time t_2.

3.3 | Calculation of Material Impact Force and Impact Moment

During the throwing process, the material binding mass can be regarded as the material binding mass remaining on the screen during the material movement time. Therefore, when the impact force of the material on the screen panel is considered, the material binding mass m_3 can be obtained as

27671402, 2025, 3, Downloaded from https://onlinelibrary.wiley.com/doi/10.1002/msd2.70010 by CochraneChina, Wiley Online Library on [11/12/2025]. See the Terms and Conditions (https://onlinelibrary.wiley.com/terms-and-conditions) on Wiley Online Library for rules of use; OA articles are governed by the applicable Creative Commons License

$$m_3 = \frac{Q_h \Delta t}{3600}\left[F_c^r E_c + F_f^r (E_c - \eta)\right] \times 1000, \tag{29}$$

where Q_h represents the screen processing capacity, $\triangle t$ is the time for which the material remains on the screen surface from the feed end to the discharge end, F_c^r and F_f^r denote the proportions of coarse and fine particles in the feed, respectively, E_c and E_f are the placement efficiencies of the coarse and fine particles, respectively, and η is the screening efficiency.

Because it is not easy to measure the thickness of the material on the screen, its average thickness is considered as the approximate thickness. The screen surface of the vibrating flip-flow screen is curved, so the material on the screen is differentiated by the angle of the screen face to facilitate calculation. Thus, the mass of the microelement material block is given by

$$\mathrm{d}m = \frac{m_3}{\delta}\mathrm{d}\alpha, \tag{30}$$

where m_3 is the material mass on the screen surface and δ is the angle between the feed end and the discharge end of the vibrating flip-flow screen.

Assuming that the collision between the material and the screen surface is inelastic and the collision time is very short, the impact force of the microelement material block on the screen at the end of the throwing motion can be obtained from the theorem of momentum.

$$\begin{cases} \mathrm{d}F_{x1} = \dfrac{\mathrm{d}m\Delta v_x}{\Delta t} \\ \mathrm{d}F_{y1} = \dfrac{\mathrm{d}m\Delta v_y}{\Delta t} \end{cases}, \tag{31}$$

where Δt denotes the time of the material impact screen surface process, in most actual cases $\Delta t = 0.001 \sim 0.1$ s [25–27]. Δv_x and Δv_y represent the velocity change values of the micro material in the axis direction x_1 and y_1 on the absolute coordinate system, respectively. When the material impacts the floating frame, its speed becomes the moving speed of the floating frame at that moment, and the change in the material speed can be calculated using the following equation:

$$\begin{cases} \Delta v_x = v_0 \cos\theta - B\omega \cos\theta \cos\omega(t + t_2) \\ \Delta v_y = v_0 \sin\theta - gt_2 - B\omega \sin\theta \cos\omega(t + t_2) \end{cases}. \tag{32}$$

The rotation of the floating frame around its center of mass is small, so the rotation of the vibrating flip-flow screen around the center of mass is considered. Then, the impact force of the material uniformly distributed on the screen surface produces a torque at the center of the screen body. Taking any point on the screen surface as an example, the torque is calculated as follows:

$$\begin{cases} \mathrm{d}M_{x1} = \mathrm{d}F_x\, y_F \\ \mathrm{d}M_{y1} = \mathrm{d}F_y x_F \end{cases}, \tag{33}$$

where x_F is the distance from the horizontal force $\mathrm{d}F_x$ to the center of mass and y_F is the distance from the vertical force $\mathrm{d}F_y$ to the center of mass.

As shown in Figure 7, since the screen has an approximately circular arc shape, SolidWorks can be used to find the center of mass location of the vibrating flip-flow screen O_1, the angle α_1 between the line connecting the center of mass to the discharge end and the center of the circle, and the radius R_1 of the center of mass.

The position relationship between the center of mass of the vibrating flip-flow screen and the impact point of the material is shown in Figure 8.

In Figure 8, O_2 represents the centroid position of the vibrating flip-flow screen, O_1 is the center of the circle of the screen, R is the arc radius of the floating frame, and R_1 is the distance from the position of the centroid of the vibrating flip-flow screen to

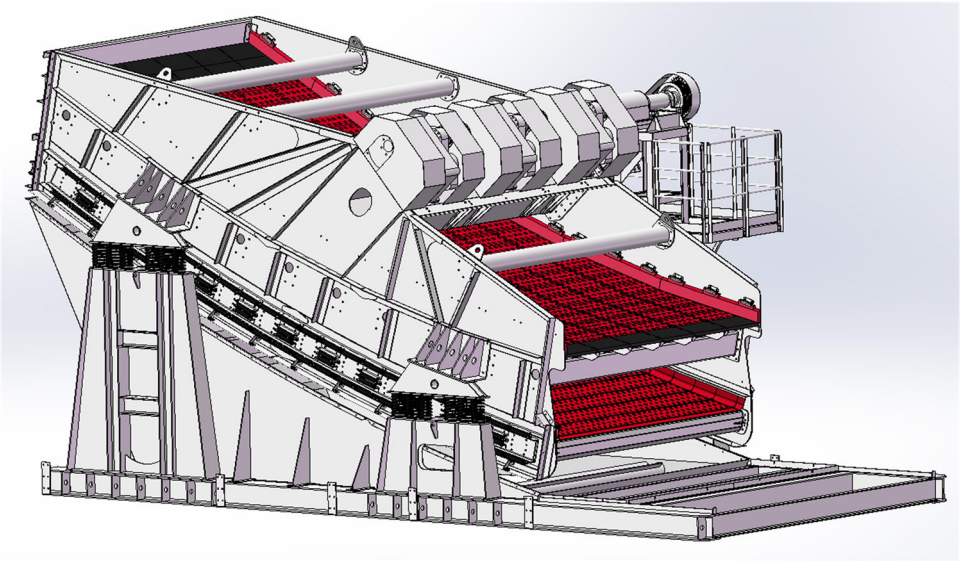

FIGURE 7 | Schematic diagram of the 3D model of a vibrating flip-flow screen.

27671402, 2025, 3, Downloaded from https://onlinelibrary.wiley.com/doi/10.1002/msd2.70010 by CochraneChina, Wiley Online Library on [11/12/2025]. See the Terms and Conditions (https://onlinelibrary.wiley.com/terms-and-conditions) on Wiley Online Library for rules of use; OA articles are governed by the applicable Creative Commons License

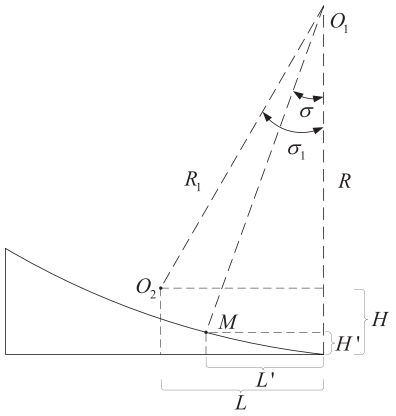

FIGURE 8 | Location diagram of the center of mass and the impact force point.

O_1. σ denotes the angle formed by the force application point and the line connecting the discharge end to the circle center and σ_1 is the angle between the centroid position and the line connecting the discharge end to the circle center.

The distance between the impact force point and the center of mass can be calculated from

$$\begin{cases} x_F = L - L' = R_1 \sin\sigma_1 - R\sin\sigma \\ y_F = H - H' = R\cos\sigma - R_1\cos\sigma_1 \end{cases}. \tag{34}$$

The impact force and the impact moment of the material can be calculated as follows:

$$\begin{cases} \mathrm{d}F_{x1} = \dfrac{m_3(v_0\cos\theta - B\omega\cos\theta\cos\omega(t+t_2))}{\delta\Delta t}\mathrm{d}\alpha \\ \mathrm{d}F_{y1} = \dfrac{m_3(v_0\sin\theta - gt_2 - B\omega\sin\theta\cos\omega(t+t_2))}{\delta\Delta t}\mathrm{d}\alpha \end{cases}, \tag{35}$$

$$\begin{cases} \mathrm{d}M_{x1} = \dfrac{m_3(v_0\cos\theta - B\omega\cos\theta\cos\omega(t+t_2))}{\delta\Delta t}(R\cos\sigma - R_1\cos\sigma_1)\mathrm{d}\alpha \\ \mathrm{d}M_{y1} = \dfrac{m_3(v_0\sin\theta - gt_2 - B\omega\sin\theta\cos\omega(t+t_2))}{\delta\Delta t}(R_1\sin\sigma_1 - R\sin\sigma)\mathrm{d}\alpha \end{cases}. \tag{36}$$

Since the above equations are only the impact force and moment of a single microelement material block, in order to find the effect of the whole material on the floating frame, the differential impact force and differential moment need to be integrated, and the components of the impact force F_{x1}, and F_{y1} and impact moment M_{x1}, and M_{y1} of the material can be obtained using the equations

$$\begin{cases} F_{x1} = \displaystyle\int_0^{\delta} \frac{m_3(v_0\cos\theta - B\omega\cos\theta\cos\omega(t+t_2))}{\delta\Delta t}\mathrm{d}\alpha \\ F_{y1} = \displaystyle\int_0^{\delta} \frac{m_3(v_0\sin\theta - gt_2 - B\omega\sin\theta\cos\omega(t+t_2))}{\delta\Delta t}\mathrm{d}\alpha \end{cases}, \tag{37}$$

$$\begin{cases} M_{x1} = \displaystyle\int_0^{\delta} \frac{m_3(v_0\cos\theta - B\omega\cos\theta\cos\omega(t+t_2))}{\delta\Delta t}(R\cos\sigma - R_1\cos\sigma_1)\mathrm{d}\alpha \\ M_{y1} = \displaystyle\int_0^{\delta} \frac{m_3(v_0\sin\theta - gt_2 - B\omega\sin\theta\cos\omega(t+t_2))}{\delta\Delta t}(R_1\sin\sigma_1 - R\sin\sigma)\mathrm{d}\alpha \end{cases}, \tag{38}$$

where δ is the angle corresponding to the line between the inlet and the outlet end of the vibrating flip-flow screen and the center of the circle.

4 | Simulation of the Vibrating Flip-Flow Screen System Considering the Material Impact Force

As previously mentioned, the coordinate system *xoy* is defined on the screen. The *x* direction is the working direction of the screen panel and the *y* direction is perpendicular to the working face. The material impact force in this coordinate system has the following components:

$$\begin{cases} F_x = F_{x1}\cos\gamma + F_{y1}\sin\gamma \\ F_y = F_{x1}\sin\gamma - F_{y1}\cos\gamma \end{cases}, \tag{39}$$

where γ is the installation angle of the vibrating flip-flow screen. The torque caused by the impact of the material on the system is given by

$$M_1 = M_{x1} + M_{y1}. \tag{40}$$

Parameters of the vibrating flip-flow screen system are shown in Table 1.

F_x, F_y, and M_1 can be calculated as shown in Figure 9.

The impact force F_x, F_y and impact moment M_1 generated by material movement have periodicity. The maximum F_x and F_y values of the material impact force are 29% and 57.58%, respectively, compared with the amplitude A of the excitation force of the vibrating flip-flow screen. It can be seen that the impact force generated by the material should be considered in the analysis and design process of the vibrating flip-flow screen.

The floating frame and the fixed beam of the main frame are alternately arranged and connected by screen panels, and therefore, the material impact force affects both. The material impact force is assumed to be equally distributed among them. Therefore, the generalized force $\boldsymbol{F}$ of the 5DOF vibration system of the vibrating flip-flow screen affected by the material impact force is expressed as

$$\boldsymbol{F} = [P\cos\beta + F_x/2 \quad P\sin\beta + F_y/2 \quad F_x/2 \quad F_y/2 - Pl_1 + M_1]^{\mathrm{T}}. \tag{41}$$

27671402, 2025, 3, Downloaded from https://onlinelibrary.wiley.com/doi/10.1002/msd2.70010 by CochraneChina, Wiley Online Library on [11/12/2025]. See the Terms and Conditions (https://onlinelibrary.wiley.com/terms-and-conditions) on Wiley Online Library for rules of use; OA articles are governed by the applicable Creative Commons License

TABLE 1 | Parameters of the vibrating flip-flow screen system.

Symbol	Unit	Parameter	Value
γ	°	Installation angle	22
β	°	Angle of excitation force	64
n	$r{\cdot}min^{-1}$	Operating speed	813
m_1	kg	Mass of the main frame	24 751.96
m_2	kg	Mass of the floating frame	3666.306
m	kg	Mass of the material	6000
l_1	m	Distance from the center of mass to the excitation force line	0.0564
l_2	m	Horizontal distance from the main frame's centroid to the vibration isolation spring	2.3679
k_x	$N{\cdot}m^{-1}$	Horizontal stiffness of the isolation spring	4.3×10^6
k_y	$N{\cdot}m^{-1}$	Vertical stiffness of the isolation spring	8.6×10^6
k_{2x}	$N{\cdot}m^{-1}$	Shear stiffness of rubber springs	3.511×10^6
k_{3x}	$N{\cdot}m^{-1}$	Flexural stiffness of the screen panels	1.2×10^6
c_{1x}	kN·s/m	Damping coefficient of isolation springs	0.01
c_{2x}	kN·s/m	Damping coefficient of rubber springs	0.03
c_{3x}	kN·s/m	Damping coefficient of screen panels	0.03
η		Material binding coefficient	0.2

In order to further analyze the influence of material impact force on the dynamic characteristics of the vibrating flip-flow screen, the Runge–Kutta method is used to numerically integrate the dynamic equation. The curves of the displacement of the vibrating flip-flow screen and the overall rotation angle as a function of time with or without the material impact force are given. The displacements of the main frame are shown in Figure 10.

As shown in Figure 10, comparing the displacement x_1 of the main frame, it can be found that the steady-state amplitude of the main frame is 2.30 mm when the effect of the material impact force is not considered. When the effect of the material impact force is considered, the vibration curve of the main frame shifts 7.94 mm in the positive direction of x_1 due to the continuous impact force. The maximum and minimum displacement values of the main frame are 10.47 and 5.41 mm, respectively. The vibration amplitude is 2.53 mm, which increases by 10% compared with that without the impact force. Compared with the displacement y_1, it can be found that when the impact force is considered, the deviation of the vibration curve in the negative direction is 12.65 mm, the maximum and minimum values of the main frame are—18.23 and −7.07 mm, respectively, and the vibration amplitude is 5.58 mm, which increases by 2.95% compared with the case without material impact.

It can be found that the effect of material impact force in the direction of x_1 is significantly greater than that in the direction of y_1. When the impact force is considered, the vibration of the main frame in the x_1 direction is more intense and unstable in the transient response stage and the vibration amplitude in the y_1 direction is less affected by the impact force, but more stable in the transient response stage. The material impact force will cause the vibration curve to offset, and therefore, the actual design should take into account the material impact force caused by the main frame at the initial stage of larger vibration amplitude and offset, to improve system durability and avoid damage (Figure 11).

The displacement x_2 of the floating frame affected by the impact force of the material increases 48.85% compared with that without the impact force, and an upward offset of 0.93 mm is generated. The displacement y_2 of the floating frame also produced a negative orientation offset of 0.44 mm, and its amplitude is 0.92 mm, which represents an increase of 84% over the unaffected value. At the same time, the cyclical peak caused by smaller shocks appears on the curve, which is 39.09% of the amplitude.

It can be seen that the material impact has a significant effect on the floating frame, which causes the floating frame to produce a large vibration amplitude in the transient response stage and the offset in the running stage. Displacements x_2 and y_2 of the floating frame are important parameters in the design of the vibrating flip-flow screen. In order to prevent large displacement caused by material impact, the stiffness of the shear spring should be appropriately increased.

To understand the motion state of the main frame and the floating frame more clearly, the centroids of the main frame and the floating frame are selected as feature points, and the motion trajectories of feature points in the stable state of the vibrating flip-flow screen system are given, when the material impact force is considered, as shown in Figure 12.

The influence of material impact force on the overall rotation angle of the vibrating flip-flow screen is shown in Figure 13. When impacted by the material, the overall shift is -3.386×10^{-2} rad. The maximum and minimum of rotation angle φ are 3.386×10^{-2} rad and -3.915×10^{-2} rad, respectively, with a 346.7% increase in amplitude.

27671402, 2025, 3, Downloaded from https://onlinelibrary.wiley.com/doi/10.1002/msd2.70010 by CochraneChina, Wiley Online Library on [11/12/2025]. See the Terms and Conditions (https://onlinelibrary.wiley.com/terms-and-conditions) on Wiley Online Library for rules of use; OA articles are governed by the applicable Creative Commons License

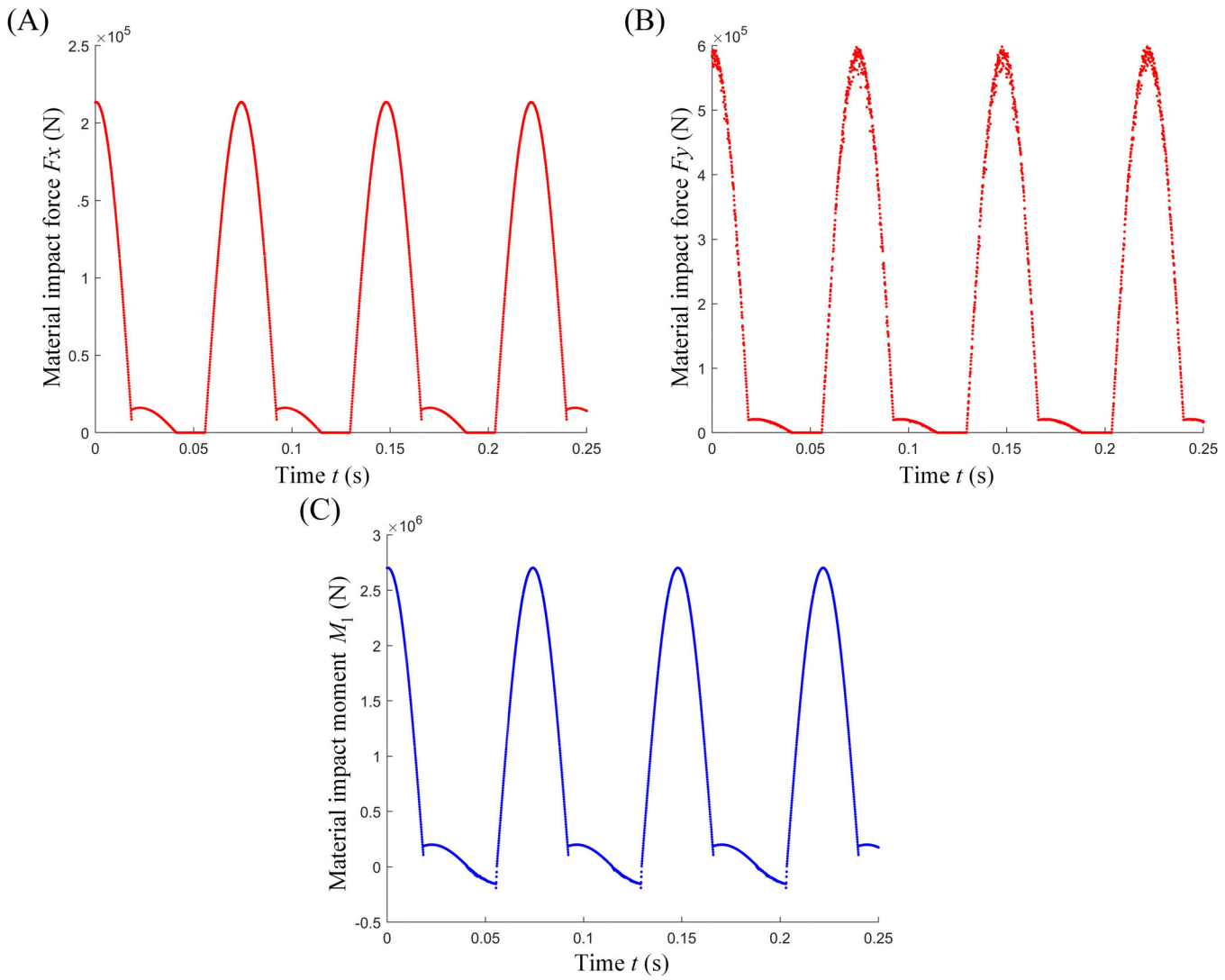

FIGURE 9 | Material impact force and impact moment as a function of time: (A) impact force F_x, (B) impact force F_y, and (C) impact torque M_1.

5 | Influence of Impact Parameters on Dynamic Characteristics

The dynamic characteristics of the vibrating flip-flow screen are affected by many factors [28–30], and the change of parameters in the working process leads to a change in the amplitude of the screen body, which may lead abnormal behavior. Therefore, it is necessary to analyze the dynamic characteristics of the vibrating flip-flow screen when various system parameters change, so as to avoid instability or even damage caused by changes in system parameters during operation. In the following subsection, the effect of different parameters is examined.

5.1 | Effect of Material Mass Variations on System Characteristics

When screening wet or fine-grained materials, there may be accumulation of materials during operation, which causes the mass of the material of the vibrating flip-flow screen system to increase, and the impact force generated by the material will change. Stopping the feed will lead to a reduction in the material on the screen, thus reducing the vibration mass. These conditions will have an effect on the dynamic characteristics of the vibrating flip-flow screen system, and for this reason, the material mass changes are analyzed as follows:

When the mass m of the material is 5000, 6000, and 7000 kg, respectively, the frequency–amplitude curves of the main frame and the floating frame are shown in Figure 14.

The amplitude of the floating frame is significantly affected by impact force before the first natural frequency, and its amplitude is much larger than that without considering impact force, while the main frame is less affected by material impact force. With an increase of the material mass on the screen, the amplitudes of the main frame and the floating frame increase, and the second natural frequency of the amplitude–frequency curve in the x_1 direction of the main frame and the x_2 direction of the floating frame decreases significantly compared with the first natural frequency.

Taking the operating frequency of the screen as a reference, the changes of the displacement x_1 of the main frame are 11.64%, 13.04%, and 14.34%, respectively, when the material impact is considered and the mass is 5000, 6000, and 7000 kg, respectively.

27671402, 2025, 3, Downloaded from https://onlinelibrary.wiley.com/doi/10.1002/msd2.70010 by CochraneChina, Wiley Online Library on [11/12/2025]. See the Terms and Conditions (https://onlinelibrary.wiley.com/terms-and-conditions) on Wiley Online Library for rules of use; OA articles are governed by the applicable Creative Commons License

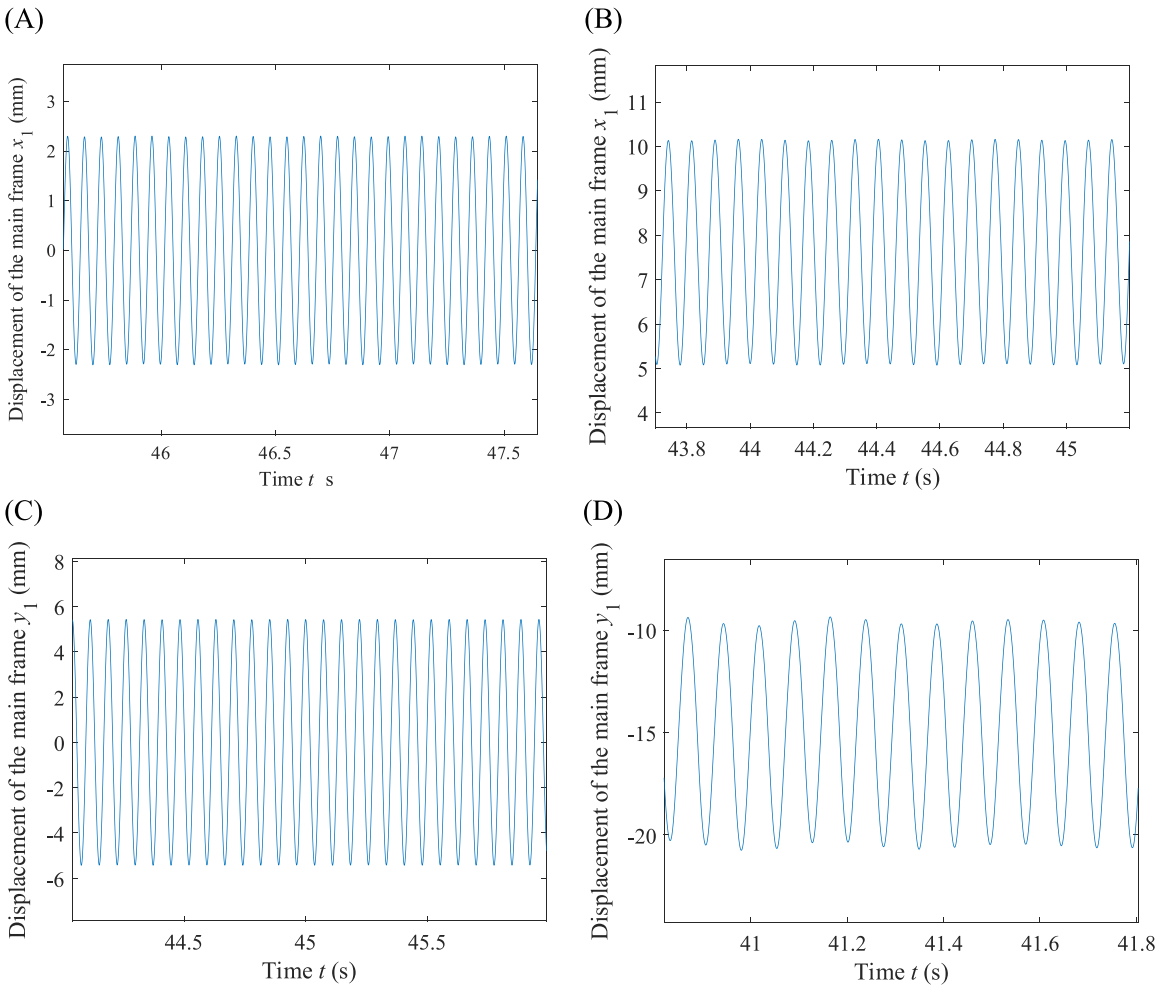

FIGURE 10 | Comparison of displacement of the main frame: (A) Displacement in the x_1 direction without considering material effects, (B) displacement in the x_1 direction considering material effects, (C) displacement in the y_1 direction without considering material effects, and (D) displacement in the y_1 direction considering material effects.

The changes of displacement y_1 of the main frame are 6.49%, 7.03%, and 8.95%. The changes of displacement x_2 of the floating frame are 19.29%, 32.39%, and 46.16%. The changes of y_2 displacement of the floating screen frame are 85.46%, 111.21%, and 137.13%. It can be seen that with the change of material mass, the sensitivities are y_1, x_1, x_2, and y_2 from small to large, respectively. The displacement y_2 of the floating frame with respect to the main frame is affected the most.

5.2 | Effect of Variations in the Material Binding Coefficient on System Characteristics

In actual conditions, various factors, such as material properties, angle of the screen, material thickness, and material shape, cause the material on the screen to have different material binding coefficients [31]. This, in turn, affects the vibration mass of the material and the impact force that it exerts. Figure 15 illustrates the influence of different material binding coefficients on the characteristics of the system considering the material impact force.

With an increase in the material binding coefficient, the amplitudes of all degrees of freedom of the vibrating flip-flow screen increase. The first-order natural frequency of the amplitude–frequency curve is less affected and the second-order natural frequency of x_1 and x_2 decreases with an increase of the material binding coefficient.

Consider the operating frequency as the reference when the material binding coefficient is 0.2, 0.3, and 0.4. The changes of x_1 and y_1 are 13.04%, 22.02%, and 35.78%, and 7.03%, 9.97%, and 15.17%, respectively. The changes of x_2 and y_2 of the floating frame displacement are 32.39%, 77.08%, 131.43%, and 111.21%, 188.62%, and 270.58%, respectively. It can be found that the sensitivities are y_1, x_1, x_2, and y_2 from small to large when the material binding coefficient is changed, and the floating frame displacement y_2 is mostly affected.

5.3 | Effect of Material Acceleration on System Characteristics

The initial acceleration of the material is provided by both the movement of the screen body and the flip-flow motion of flip-flow screen panels, with the flip-flow motion serving as the primary contributing factor. It is influenced by both the physical parameters of the screen panels as well as factors such as

27671402, 2025, 3, Downloaded from https://onlinelibrary.wiley.com/doi/10.1002/msd2.70010 by CochraneChina, Wiley Online Library on [11/12/2025]. See the Terms and Conditions (https://onlinelibrary.wiley.com/terms-and-conditions) on Wiley Online Library for rules of use; OA articles are governed by the applicable Creative Commons License

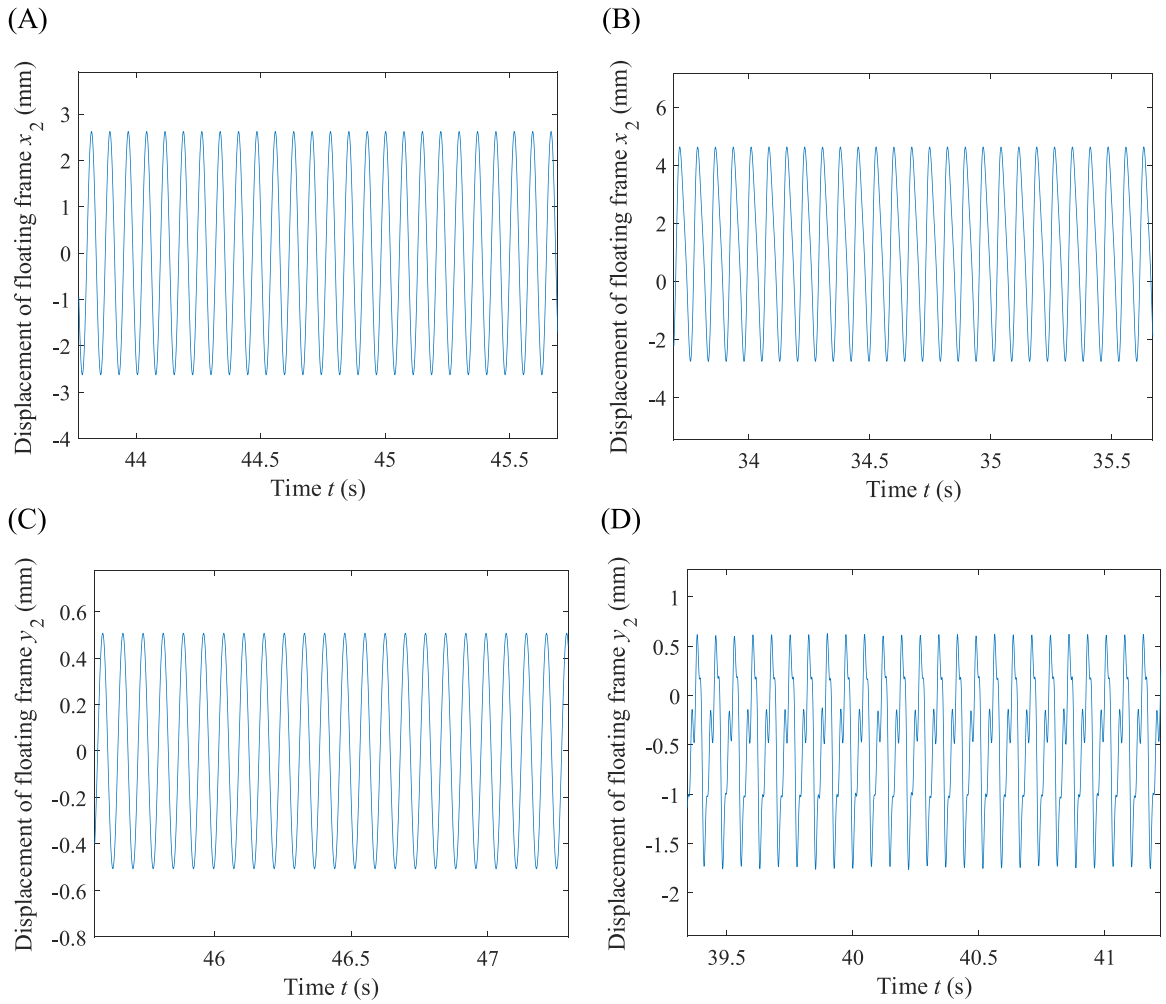

FIGURE 11 | Comparison of displacement of the floating frame: (A) Displacement in the x_2 direction without considering material effects, (B) displacement in the x_2 direction considering material effects, (C) displacement in the y_2 direction without considering material effects, and (D) displacement in the y_2 direction considering material effects.

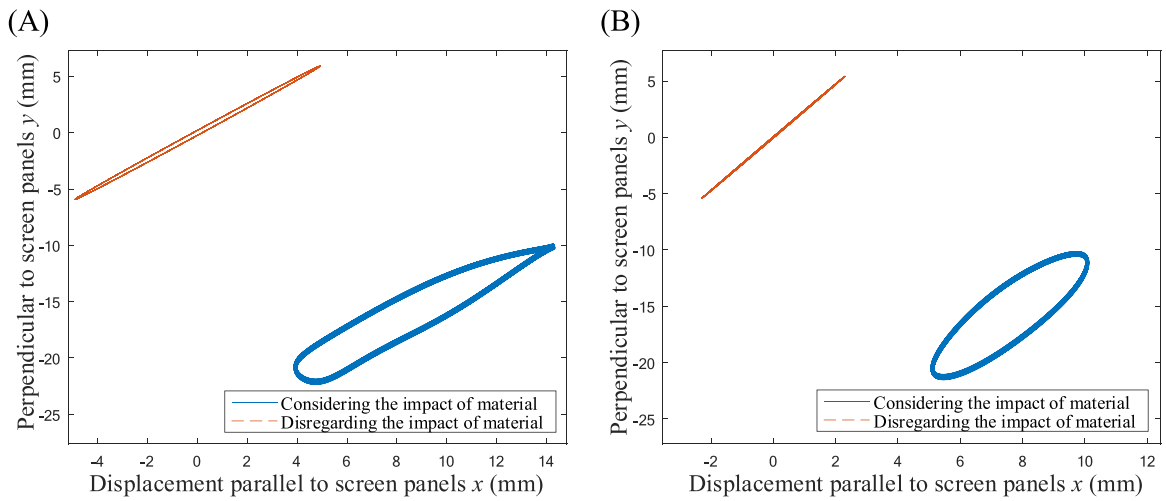

FIGURE 12 | Center of mass motion trajectory: (A) floating frame and (B) main frame.

material properties and layer thickness. Hence, an analysis of the system characteristics, taking into account the material impact force under varying material acceleration scenarios, is performed, and the results are shown in Figure 16.

An examination of the results of Figure 16 indicates that an increase in material acceleration results in significant amplification of the amplitudes, particularly at lower frequencies, across the various degrees of freedom of the flip-flow screen.

27671402, 2025, 3, Downloaded from https://onlinelibrary.wiley.com/doi/10.1002/msd2.70010 by CochraneChina, Wiley Online Library on [11/12/2025]. See the Terms and Conditions (https://onlinelibrary.wiley.com/terms-and-conditions) on Wiley Online Library for rules of use; OA articles are governed by the applicable Creative Commons License

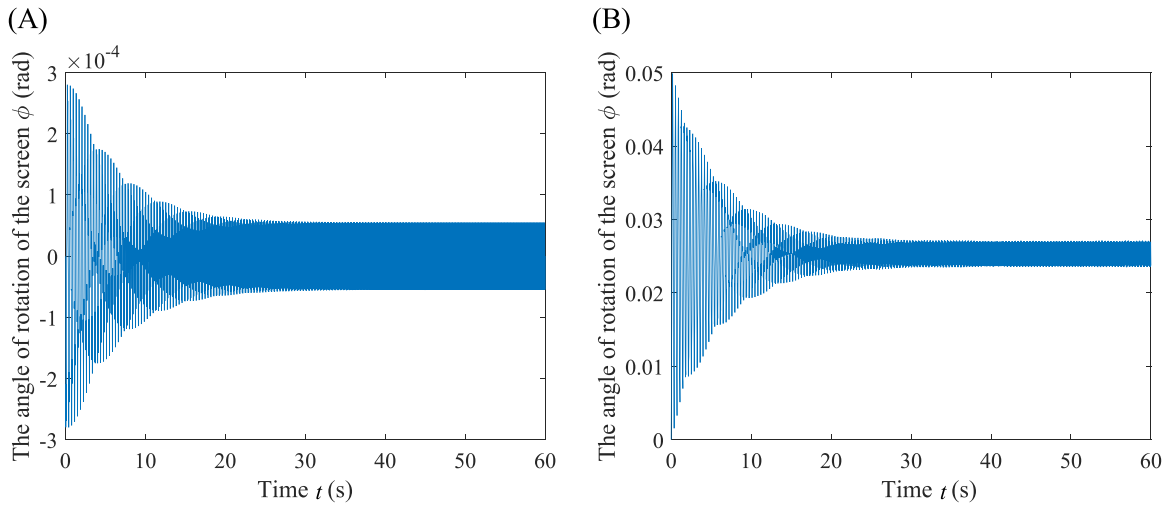

FIGURE 13 | Overall rotation angle φ of the vibrating flip-flow screen: (A) without considering material effects and (B) considering material effects.

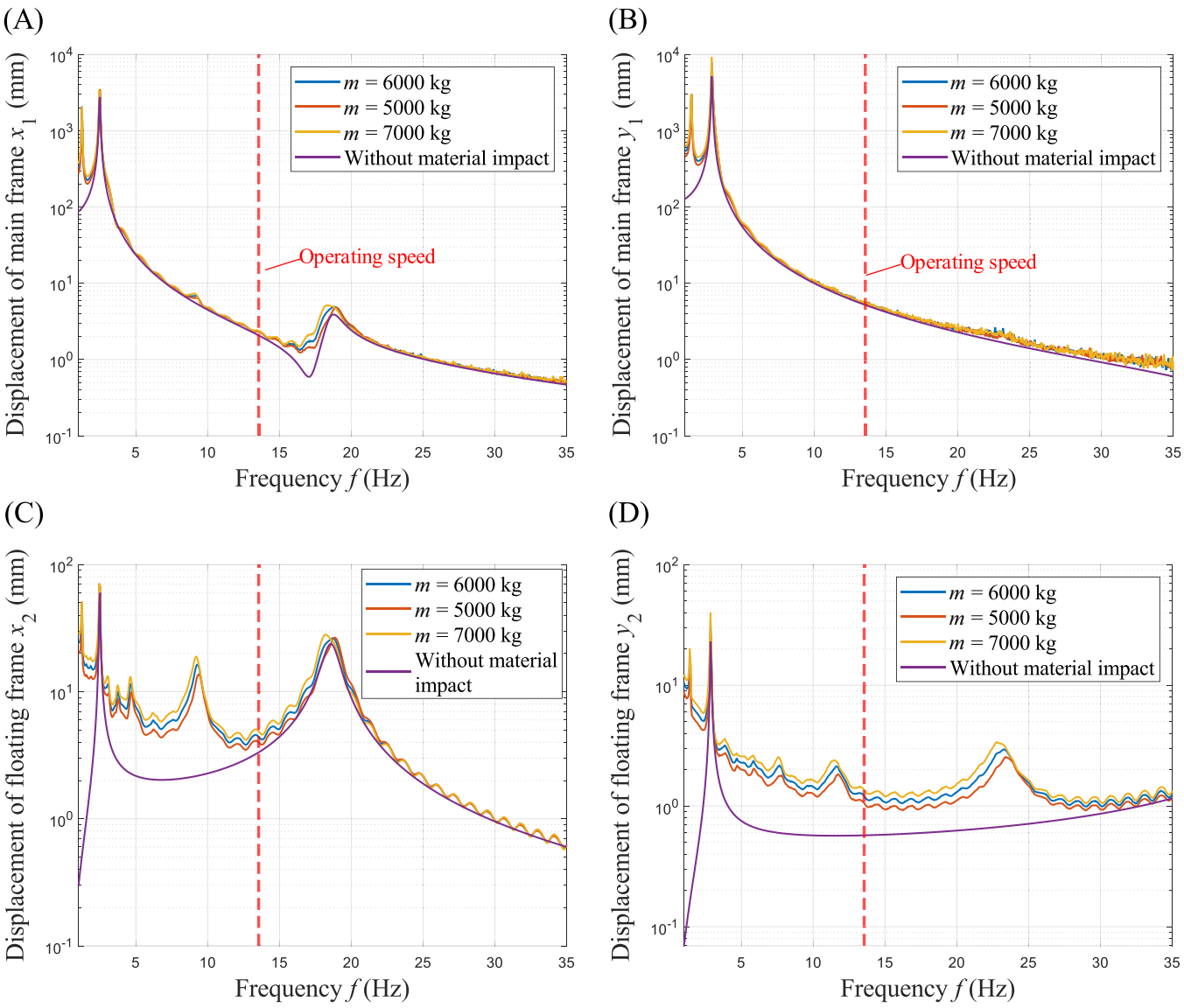

FIGURE 14 | Amplitude–frequency curve of the vibrating flip-flow screen: (A) displacement of the main frame x_1, (B) displacement of the main frame y_1, (C) displacement of the floating frame x_2, and (D) displacement of the floating frame y_2.

27671402, 2025, 3, Downloaded from https://onlinelibrary.wiley.com/doi/10.1002/msd2.70010 by CochraneChina, Wiley Online Library on [11/12/2025]. See the Terms and Conditions (https://onlinelibrary.wiley.com/terms-and-conditions) on Wiley Online Library for rules of use; OA articles are governed by the applicable Creative Commons License

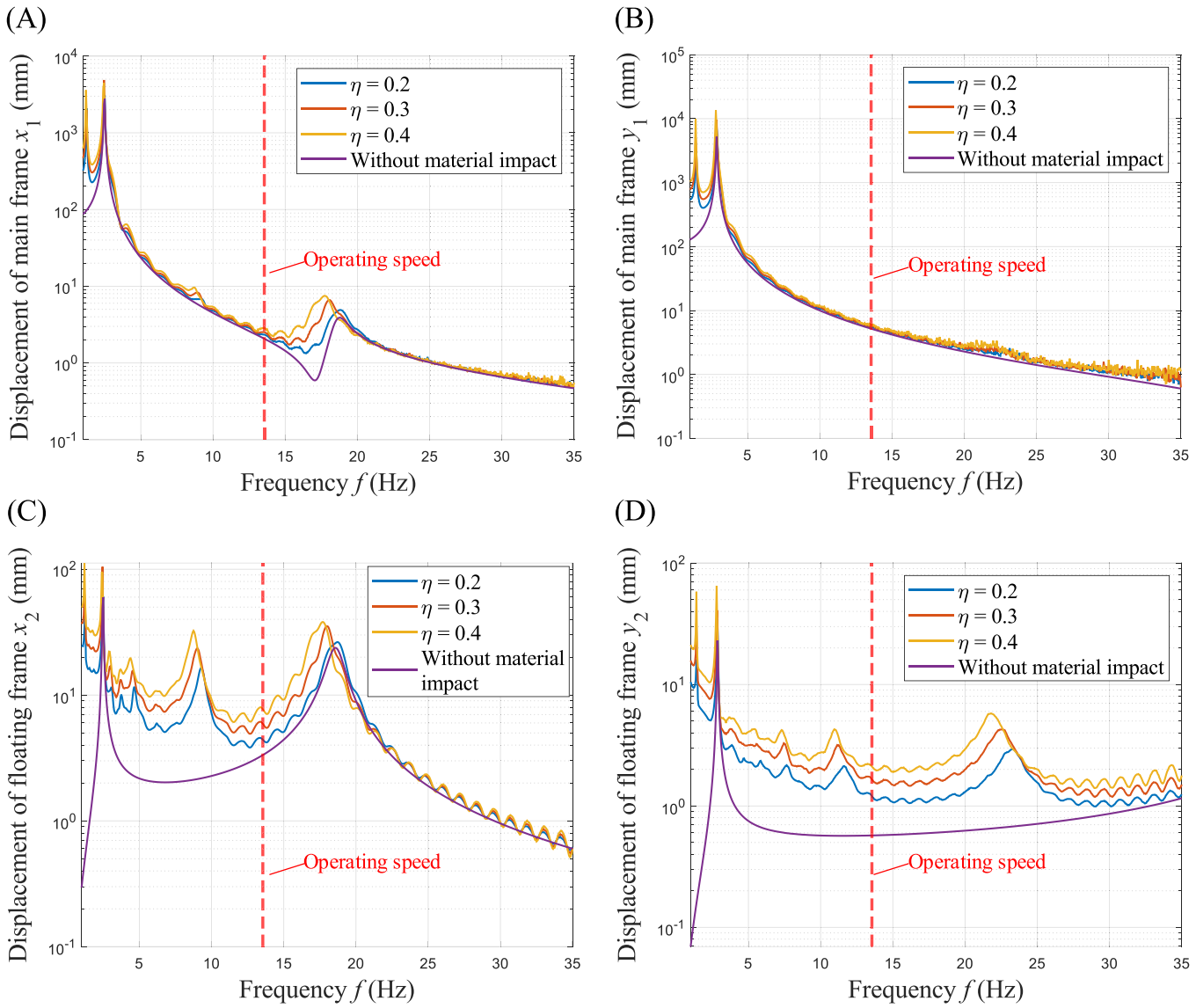

FIGURE 15 | Amplitude–frequency curve of the vibrating flip-flow screen: (A) displacement of the main frame x_1, (B) displacement of the main frame y_1, (C) displacement of the floating frame x_2, and (D) displacement of the floating frame y_2.

At the operating frequency of the flip-flow screen, the percentage changes in the displacement of the main frame x_1 are 10.63%, 13.04%, and 18.69%. The percentage changes in the displacement y_1 are 6.41%, 7.05%, and 13.02%. Similarly, the percentage changes in the displacement of the floating frame x_2 are 18.15%, 32.39%, and 47.84% and the percentage changes in the displacement y_2 are 74.08%, 111.21%, and 151.31%.

In summary, the analysis indicates that the sensitivity of the degrees of freedom of the flip-flow screen to different impact parameters, in descending order, is as follows: material binding coefficient, material acceleration, and material mass. When the impact parameters of the flip-flow screen change, the amplitude of the displacement y_2 of the floating frame relative to the main frame in the direction perpendicular to the working direction is most significantly affected. Therefore, when designing the flip-flow screen, the effect of changes in impact parameters should be considered, and attention should be paid to whether the displacement y_2 of the floating frame relative to the main frame in the direction perpendicular to the working direction exceeds the design requirements as a result. Additionally, it has been observed that variations in the material mass and the material binding coefficient can lead to changes in the system natural frequencies, resulting in significant amplitude fluctuations not only before the first natural frequency of the main frame but also within the frequency ranges of 5–10 Hz and 20–25 Hz for the floating frame. When selecting the operating frequency, it is important to avoid these peak values to prevent adverse impacts on the working efficiency and lifespan of the flip-flow screen.

6 | Conclusion

This paper conducted a dynamic characteristic analysis of the vibrating flip-flow screen, considering the impact force of the material. A dynamic model of the vibrating flip-flow screen that incorporates the impact force of the material was developed. The motion of the material on the screen was analyzed, and calculations of the material impact force and impact moment

27671402, 2025, 3, Downloaded from https://onlinelibrary.wiley.com/doi/10.1002/msd2.70010 by CochraneChina, Wiley Online Library on [11/12/2025]. See the Terms and Conditions (https://onlinelibrary.wiley.com/terms-and-conditions) on Wiley Online Library for rules of use; OA articles are governed by the applicable Creative Commons License

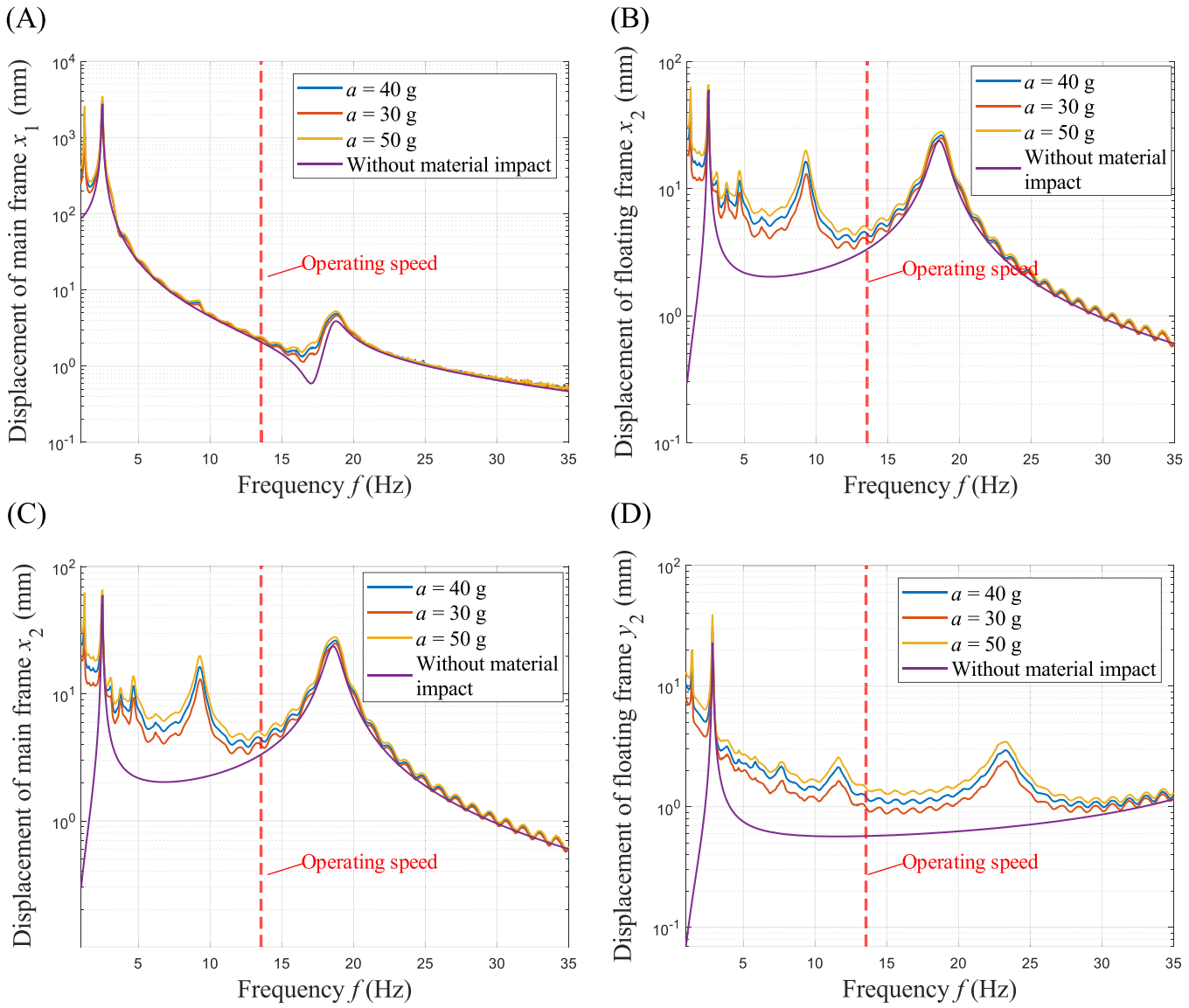

FIGURE 16 | Amplitude–frequency curve of the vibrating flip-flow screen: (A) displacement of the main frame x_1, (B) displacement of the main frame y_1, (C) displacement of the floating frame x_2, and (D) displacement of the floating frame y_2.

were carried out. The effects of different parameters on the dynamic characteristics of the vibrating flip-flow screen were also analyzed. The main conclusions are as follows:

1. After calculating and comparing the compressive stiffness and the shear stiffness of the shear springs in the vibrating flip-flow screen, it was found that the compressive stiffness of the shear springs is only 8.525 times that of its shear stiffness. Therefore, when developing the dynamic model of the vibrating flip-flow screen, the vertical displacement of the floating frame relative to the main frame should be taken into consideration.

2. An analysis was conducted on the material motion on the vibrating flip-flow screen, during which the initial velocity of the material was calculated. Furthermore, the impact forces and moments exerted by the material on the vibrating flip-flow screen were derived and their time-varying curves were plotted. The results revealed that the material impact forces F_x and F_y account for 29% and 57.58% of the amplitude of the excitation force, respectively, indicating that they are of the same order of magnitude as the excitation force. Therefore, the influence of material impact forces should not be neglected in the design and calculation of flip-flow screens.

3. Based on the impact forces, a dynamic characteristic analysis of the vibrating flip-flow screen was conducted. A comparative analysis was performed between two scenarios: one considering the impact forces and the other neglecting these. The findings indicated that the material impacts result in increased displacements across all degrees of freedom of the vibrating flip-flow screen. Additionally, the displacement curves of both the main frame and the floating frame showed shifts. Notably, the material impact forces have a relatively significant influence on the amplitude and the relative amplitude of the floating frame.

4. The degree of influence of different parameters on the degrees of freedom of the vibrating flip-flow screen, from the greatest to the least, is the material binding coefficient,

27671402, 2025, 3, Downloaded from https://onlinelibrary.wiley.com/doi/10.1002/msd2.70010 by CochraneChina, Wiley Online Library on [11/12/2025]. See the Terms and Conditions (https://onlinelibrary.wiley.com/terms-and-conditions) on Wiley Online Library for rules of use; OA articles are governed by the applicable Creative Commons License

material acceleration, and material mass. The greatest impact due to all parameters in terms of perpendicularity to the working direction occurs in the floating frame relative to the main frame. The increase in both the material mass and the material binding coefficient leads to a decrease in the natural frequencies of the system. The amplitude–frequency curve of the main frame peaks before the first order of the intrinsic frequency and the amplitude–frequency curve of the floating frame peaks at intervals of 5–10 Hz and 20–25 Hz. The actual force situation of the vibrating flip-flow screen is more complicated; future research can consider the friction of the material and the impact force generated during material conveying and other comprehensive force scenarios to develop a more detailed dynamic model and further study the dynamic characteristics of vibrating flip-flow screens.

Acknowledgments

This study was supported by the National Natural Science Foundation of China (Grant No. 12272259).

Conflicts of Interest

The authors declare no conflicts of interest.

Data Availability Statement

Data that support the findings of this study are available from the corresponding author upon reasonable request.

References

1. Y. Liu, "Analysis and Application of Flip-Flow Screen in Fine-Grain Raw Coal Screening Operation," *Coal Processing & Comprehensive Utilization* 275, no. 6 (2022): 25–27.

2. L. L. Zhao, H. Jiang, Y. M. Zhao, et al., "Review of Dry Screening Theory and Cross Screening Technology for Wet Cohesive Fine Coal," *Coal Science and Technology* 50, no. 10 (2022): 251–258.

3. H. Li, C. Liu, L. Shen, L. Zhao, and S. Li, "Kinematics Characteristics of the Flip-Flow Screen With a Crankshaft-Link Structure and Screening Analysis for Moist Coal," *Powder Technology* 394 (2021): 326–335.

4. Y. Z. Jiang, K. F. He, Y. L. Dong, D. Yang, and W. Sun, "Influence of Load Weight on Dynamic Response of Vibrating Screen," *Shock and Vibration* 2019, no. 1 (2019): 1–8.

5. D. Lin, J. Ji, C. Yu, X. Wang, and N. Xu, "A Non-Linear Model of Screen Panel for Dynamics Analysis of a Flip-Flow Vibrating Screen," *Powder Technology* 418 (2023): 118312.

6. D. Lin, N. Xu, C. Yu, R. Geng, X. Wang, and S. Gong, "Nonlinear Model of Vibrating Flip-Flow Screens That Considers the Effects of Screen Panels," *IEEE Access* 10 (2022): 34246–34259.

7. Z. X. He, X. Z. Wang, Z. F. Xing, and H. Xiao, "Dynamic Characteristics Analysis of Vibrating Screen Based on System and Particle Coupling Dynamics," *Journal of South China University of Technology* 51, no. 1 (2023): 41–50.

8. Z. Wang, C. Liu, J. Wu, H. Jiang, and Y. Zhao, "Impact of Screening Coals on Screen Surface and Multi-Index Optimization for Coal Cleaning Production," *Journal of Cleaner Production* 187 (2018): 562–575.

9. G. G. Zhou, Z. G. Hu, L. X. He, and Q. J. Li, "Calculation of Material Binding Coefficient and Equivalent Resistance Coefficient for Large Linear Vibrating Screens," *Coal Preparation Technology* 30, no. 4 (2002): 12–15.

10. M. Manuel Moncada and C. G. Rodriguez, "Dynamic Modeling of a Vibrating Screen Considering the Ore Inertia and Force of the Ore Over the Screen Calculated With Discrete Element Method," *Shock and Vibration* 2018, no. 1 (2018): 1714738.

11. J. Michalczyk, Ł. Bednarski, and M. Gajowy, "Feed Material Influence on the Dynamics of the Suspended Screen at Its Steady State Operation and Transient States," *Archives of Mining Sciences* 62, no. 1 (2017): 145–161.

12. Z. Wang, L. Peng, C. Zhang, L. Qi, C. Liu, and Y. Zhao, "Research on Impact Characteristics of Screening Coals on Vibrating Screen Based on Discrete-Finite Element Method," *Energy Sources, Part A: Recovery, Utilization, and Environmental Effects* 42, no. 16 (2019): 1963–1976.

13. Y. J. Hou, G. Xiong, P. Fang, Y. W. Wang, and M. J. Du, "Study on Stability of Self-Synchronous Far-Resonant Vibrating System of Two Eccentric Rotors Considering Material Impact," *Journal of Science and Technology* 35, no. 8 (2021): 3271–3279.

14. C. W. Jiao, J. Liu, F. B. Wang, and J. P. Zhang, "Dynamical Analysis of Anti-Resonance Vibrating Machine Under Material Impact," *Journal of Northeastern University* 31, no. 11 (2010): 1615–1618.

15. G. Y. Ma, *Study on Vibration Characteristics and Parameter Optimization of Double-Mass Linear Vibrating Screen* (Yanshan University, 2019), https://doi.org/10.27440/d.cnki.gysdu.2019.000079.

16. X. H. Xia, L. X. Gou, Z. L. Zhang, et al., "Collaborative Optimization of Linear Vibrating Screen Screening Efficiency and Dynamic Response Stability Based on Coupled DEM-MBK Simulation," *Particuology* 78 (2023): 49–61.

17. L. Li, H. Zhang, and H. Zhong, "Time-Varying Piecewise Nonlinear Dynamic Model of the Vibrating Machinery With Elliptical Trajectory Consider the Interactions Between Its Frame and Particles," *International Journal for Numerical Methods in Engineering* 123, no. 20 (2022): 4778–4808.

18. D. Lin, J. C. Ji, X. Wang, et al., "A Rigid-Flexible Coupled Dynamic Model of a Flip-Flow Vibrating Screen Considering the Effects of Processed Materials," *Powder Technology* 427 (2023): 118753.

19. L. Peng, Z. Wang, W. Ma, X. Chen, Y. Zhao, and C. Liu, "Dynamic Influence of Screening Coals on a Vibrating Screen," *Fuel* 216 (2018): 484–493.

20. B. C. Wen, S. Y. Liu, and X. L. Zhang, *Theory and Method of Innovative Design for Vibrating Machinery* (Machinery Industry Press, 2021).

21. B. C. Wen and S. Y. Liu, *Modern Vibrating Screening Technology and Equipment Design* (Metallurgical Industry Press, 2013).

22. B. Csizmadia, A. Hegedűs, and I. Keppler, "Optimization of a Vibrating Screen's Mechanical Parameters," in *IUTAM Symposium on Dynamics Modeling and Interaction Control in Virtual and Real Environments, IUTAM Bookseries*, vol. 30, ed. G. Stepan, L. L. Kovacs, and A. Toth (Springer, 2011), 145–152, https://doi.org/10.1007/978-94-007-1643-8_17.

23. H. X. Li, *Study on Dynamics and Screening Characteristics of Flip-Flow Screen With Crankshaft-Link Structure* (China University of Mining and Technology, 2022), https://doi.org/10.27623/d.cnki.gzkyu.2022.000021.

24. M. Q. Zou, *Dynamics Parameter Design and Kinematics Characteristics Analysis of Unilateral Driven Flip-Flow Screen* (China University of Mining and Technology, 2018), https://kns.cnki.net/kcms2/article/abstract?v=SmerkCJHUJljIofQ12cWrNk-E-uFdXkwa2AP_c8EQAnlBCX4HgWxRIWpqwKcO8Zuvtpz6p7D06wpFmfWxpmV-GzmqGBDDrxJZ1tzDFdMVpn2nMhrWk99VkKR78sHzhyD_ms_LxAladDy1RZGGS8B9XEYDdJaIdPER9rPuZxU5iFcqYFfGQH3s1DGfc7L-CLoAnZvrWJhT-8Y=&uniplatform=NZKPT&language=CHS.

25. D. X. Cheng, *Handbook of Mechanical Design*, 5th ed. (Chemical Industry Press, 2018).

26. X. Wu, "Impact Calculation for Dynamic Load Problem Based on Considering the Effect of Damping," *Mechanics in Engineering* 36, no. 02 (2014): 219–221.

27671402, 2025, 3, Downloaded from https://onlinelibrary.wiley.com/doi/10.1002/msd2.70010 by CochraneChina, Wiley Online Library on [11/12/2025]. See the Terms and Conditions (https://onlinelibrary.wiley.com/terms-and-conditions) on Wiley Online Library for rules of use; OA articles are governed by the applicable Creative Commons License

27. X. Wang, J. P. Xian, Y. D. Wang, F. Ye, and S. Huang, "Deduction of Rockfall Impact Force Based on Dimension Reduction Concept and Dimensionless Solution," *Science Technology and Engineering* 23, no. 34 (2023): 14841–14850.

28. B. Zou, *Study on Dynamic Characteristics of Double-Layer Circular Vibrating Relaxation Screen* (China University of Mining and Technology, 2023), https://doi.org/10.27623/d.cnki.gzkyu.2023.000671.

29. K. W. Pu, X. W. Wang, N. N. Xu, et al., "Dynamic Structure Characteristic Analysis of Circular Vibrating Flip-Flow Screen," *Coal Engineering* 54, no. 6 (2022): 165–171.

30. Q. Dong, *Study on Dynamic Characteristics and Structural Optimization of Double-Layer Linear Vibrating Flip-flow Screen* (China University of Mining and Technology, 2023), https://doi.org/10.27623/d.cnki.gzkyu.2023.002038.

31. L. L. Xin, J. H. Liang, and B. C. Wen, "Dynamic Analysis of a Vibrating Conveyer With Inclination in Consideration of Material Combination Coefficient," *Transactions of the Chinese Society for Agricultural Machinery* 40, no. 2 (2009): 87–90.

27671402, 2025, 3, Downloaded from https://onlinelibrary.wiley.com/doi/10.1002/msd2.70010 by CochraneChina, Wiley Online Library on [11/12/2025]. See the Terms and Conditions (https://onlinelibrary.wiley.com/terms-and-conditions) on Wiley Online Library for rules of use; OA articles are governed by the applicable Creative Commons License